

Learning Gait Models with Varying Walking Speeds

Chaobin Zou¹, Rui Huang¹, *Member, IEEE*, Hong Cheng^{1*}, *Senior member, IEEE*, Jing Qiu²

Abstract—Lower-limb exoskeletons can reduce the therapist’s burden and quantify repetitive gait training for patients with gait impairments. For patient’s gait training, different walking speeds are required at different rehabilitation stages. However, due to the uniqueness of gait patterns, it is challenging for lower limb exoskeletons to generate individualized gait patterns for patients with different anthropometric parameters. This paper proposed learning-based gait models to learn and reconstruct gait patterns from healthy subject’s gait database, including the Gait Parameters Model (GPM) and the Gait Trajectory Model (GTM). The GPM employs Neural Networks to predict gait parameters with a given desired walking speed and the anthropometric parameters of the subject. The GTM utilizes Kernelized Movement Primitives (KMP) to reconstruct gait patterns with the predicted gait parameters. The proposed approach has been tested on a lower limb exoskeleton named AIDER. Experimental results indicate that the reconstructed gait patterns are very similar to the subject’s actual gait patterns for varying walking speeds.

Index Terms—Prosthetics and Exoskeletons, Learning from Demonstration, Motion and Path Planning.

I. INTRODUCTION

Robotic lower-limb exoskeletons are designed for rehabilitation training for patients with gait impairments suffering from post-stroke or Spinal Cord Injury (SCI). Significant achievements have been made in last decades, such as Lokomat [1], ReWalk [2], EKSO GT [3], Indego [4] and HAL [5]. These robotic exoskeletons strap to the patient’s legs and provide gait training for patients.

Walking speed is a key indicator for assessing a patient’s physical condition [6] [7], numerous researchers consider walking speed as a measurement of functional abilities [8]. Walking speed is a quick and easy test and often included in clinical and epidemiological research studies [9], timed walking tests are increasingly performed as outcome measures [10]. In the rehabilitation for patients with gait impairments (e.g., hemiplegic patients), the most important thing is to improve the walking speed and regain more mobility for their social lives [11] [12]. Usually, in the early stage of rehabilitation, a slow walking speed is required due to the little motor function and muscle force of the patient. The faster speed is required when patients regain basic mobility with the improvement of muscle force and balance [13] [14]. Therefore different walking speeds are required at different rehabilitation stages. As shown in Fig. 1, gait training with the exoskeleton on a treadmill provides variable walking

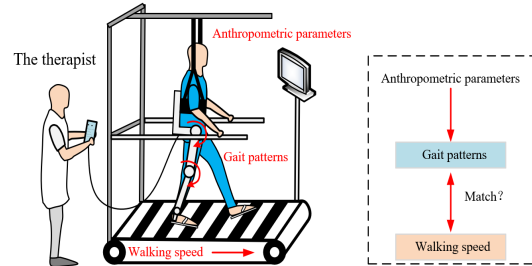


Fig. 1. A subject is gait training on the treadmill with a lower limb exoskeleton. The walking speed of the treadmill is specified by the therapist, how to generate gait patterns for the exoskeleton to match the speed?

speed training. As will be shown in this paper, walking speed is highly correlated to gait patterns and affected by anthropometric factors [15], predefined fixed gait patterns are likely not suitable for all subjects. For different subjects with varying anthropometric parameters, it is not physically feasible to design all gait patterns to match all subjects with any given walking speed.

In this paper, the gait pattern is represented by joint angles of lower limbs. To generate natural gait patterns for the lower limb exoskeleton, two critical issues need to be resolved. The first one is to find the relationship between anthropometric parameters and gait parameters, the second one is joint angles generation based on the predicted gait parameters.

For gait parameters prediction, as the gait parameters are related to many anthropometric factors such as age, gender, height, and weight, the relationship between anthropometric factors and gait parameters is nonlinear, which can not be built with an accurate mathematical function. S. Ren *et al.* [16] designed a random forest based algorithm to find relationships between anthropometric features and gait patterns, and employed minimal redundancy maximal relevance criterion to find the optimal features [17]. F. Moissenet *et al.* [18] analyzed relationships among age, gender, walking speed, and body mass index. Lim *et al.* utilized multi-layer perceptron neural networks to predict stride length and cadence for different walking states (slow/natural/fast) based on anthropometric parameters [19], but it can not predict gait parameters with a given walking speed. In this paper, the neural network is utilized to predict gait parameters based on anthropometric parameters and a given walking speed.

For joint angles generation, many trajectory fitting methods were proposed such as the Spline interpolation, Fourier series fitting, and Point-Velocity-Time (PVT) interpolation. Fourier coefficient vector and Fourier series were used for joint angles construction [20] [21]. In [20], joint angles

¹C. Zou, R. Huang and H. Cheng are with Center for Robotics, School of Automation and Engineering, University of Electronic Science and Technology of China, Chengdu, China.

²J. Qiu is with the School of Mechanical and Electrical Engineering, University of Electronic Science and Technology of China, Chengdu, China.

*H. Cheng is the corresponding author. hcheng@uestc.edu.cn

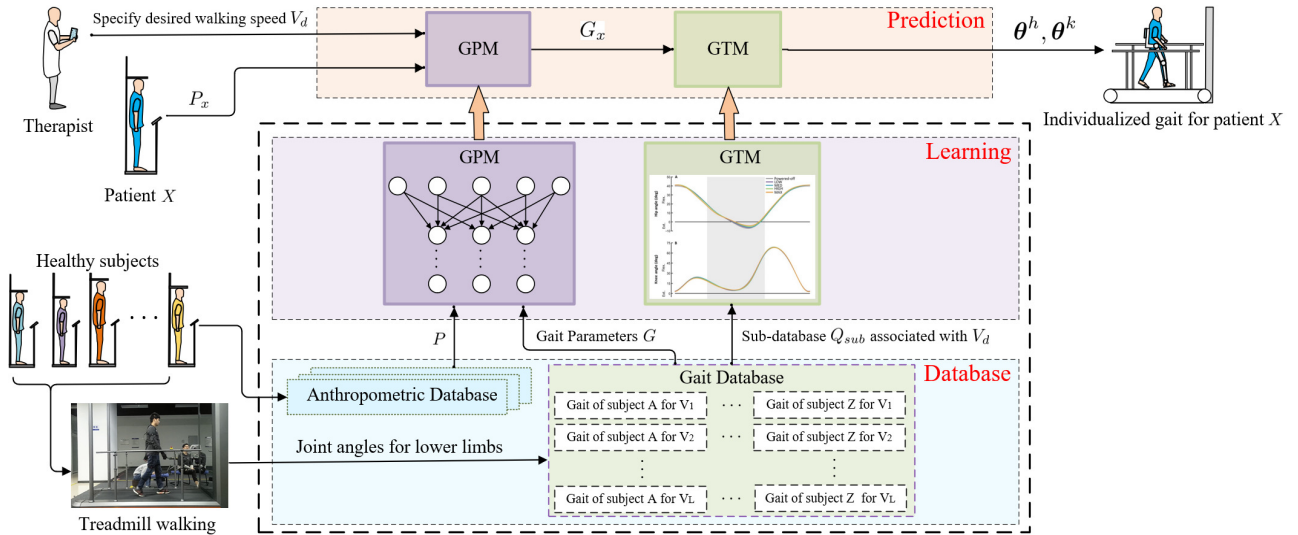


Fig. 2. The framework of the individualized gait patterns generation approach. The anthropometric database is built by anthropometric measuring from healthy subjects without gait impairments, the gait database can be built by collecting these subject's joint angles. The Gait Trajectory Model and Gait Parameters Model can be learned from these two databases. The individualized gait patterns for new subjects can be generated based on their anthropometric parameters the desired walking speed specified by the therapist.

were reconstructed at a few, fixed walking speeds based on the subject's height alone, which is undesirable as two subjects may have the same height with different leg lengths. In [21], the gait parameters (*i.e.* stride length, cadence) were specified manually for joint angle generation, but a convenient method for selecting joint angles for a given walking speed is not provided. B. Koopman *et al.* utilized Polynomial fitting to reconstruct joint angles based on the maxima and minima of the joint angle, joint angular velocity, and acceleration [22]. These approaches can not address the problem with multiple demonstrated reference trajectories. To obtain better performance for joint angles reconstruction, learning from multiple demonstrated trajectories is necessary, therefore probabilistic trajectory encoding methods can be employed. Gaussian process regression [15] [23] and Gaussian Mixture Model/Regression (GMM-GMR) [24] were used to reproduce joint angles by learning from the demonstrated database, meanwhile, joint trajectory distribution can be learned, but it is not intuitive to modify the joint angles to satisfy local fitting, such as passing through specific via-points/end-points. Probabilistic Movement Primitives (ProMP) [25] [26] formulates the modulation of trajectories as a Gaussian conditioning problem, and provides an analytical solution to modify trajectories towards via-points/end-points. Unfortunately, ProMP depends on explicit basis functions that need expensive computing processes. Huang *et al.* proposed Kernelized Movement Primitives (KMP) [27] does not require an explicit basis function definition, and allows for the creation of trajectories with specific via-points/end-points.

In this paper, learning-based gait models are proposed for gait patterns reconstruction, main contributions are threefold:

- The gait variations for different subjects with varying walking speeds have been analyzed, some via-points

were extracted as gait parameters for varying speeds.

- Learning-based gait models combine the neural networks and KMP have been proposed to reconstruct gait patterns for subjects with varying anthropometric parameters for any given walking speed.
- The proposed approach was applied to a lower limb rehabilitation exoskeleton named AIDER, the contribution and the limitation of the approach were discussed.

This study is a preliminary stage in the development process for exoskeletons and is shown valid for healthy individuals.

II. METHODS

A. The framework of the approach

As shown in Fig. 2, the overall framework consists of three parts: database, learning, and prediction.

1) *Database*: The anthropometric database and gait database for different walking speeds were collected from healthy subjects. Note that $P \in \mathbb{R}^{H \times S}$ is the anthropometric parameters database,

$$P = \{p_{s,1}, p_{s,2}, \dots, p_{s,H}\}_{s=1}^S, \quad (1)$$

where H is the number of anthropometric parameters, S is the number of subjects. $Q \in \mathbb{R}^{D \times S \times L}$ is the collected joint angles with different walking speeds,

$$Q = \{\{\theta_{s,l}^h, \theta_{s,l}^k\}_{s=1}^S\}_{l=1}^L, \quad (2)$$

where $\theta_{s,l}^h, \theta_{s,l}^k \in \mathbb{R}^N$ are hip and knee flexion/extension joint angles. N is the data length for each demonstration, L is an enumeration of the speeds assessed. $G \in \mathbb{R}^C$ is gait parameters, C is dimension of G , *i.e.*, $G = \{g_1, g_2, \dots, g_C\}$.

2) *Learning for Gait Models*: The Gait Parameters Model (GPM) is based on the neural networks, the Gait Trajectory Model (GTM) employs KMP for joint angles reconstruction. The learning process of the GPM and GTM is off-line on the gait database collected from healthy subjects.

3) *Prediction*: Prediction for a new subject X with the anthropometric parameters P_x . V_d is the desired walking speed specified by the therapist, Q_{sub} is the sub-database associated with V_d of gait database, $Q_{sub} = \{Q|V = V_d\}$. G_x is the predicted gait parameters corresponding to V_d and P_x , the individualized joint angles θ^h , θ^k for subject X can be generated by GTM based on G_x and Q_{sub} . Note that Q is collected with discrete walking speeds, and may not include V_d . For instance, $V_d = 1.3$ km/h, the nearest speeds for V_d are $V_1 = 1.0$ km/h and $V_2 = 1.5$ km/h in Q , thus the Q_{sub} is the union for both V_1 and V_2 , $Q_{sub} = Q_{V_1} \cup Q_{V_2}$.

B. Gait Parameters Model

The GPM is based on a three-layer neural network for building relationships between anthropometric parameters and gait parameters, it is learned from the database P and G . Based on the statistical analysis for gait trajectories from many subjects [15] [23], anthropometric parameters that affect gait patterns are chosen, as shown in Fig. 3 (a) and Fig. 3 (b). The correlations between these anthropometric parameters and gait parameters for different walking speeds are analyzed in Section III-B.

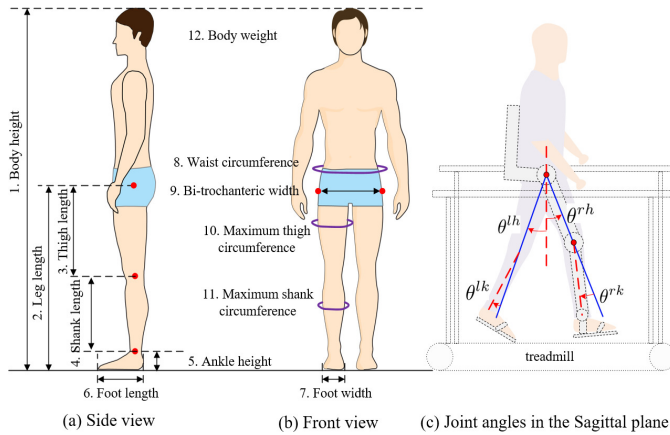


Fig. 3. The anthropometric parameters and joint angles in Sagittal plane.

The gait patterns are represented by hip and knee flexion/extension joint angles in the Sagittal plane, as shown in Fig. 3(c). The joint angles vary from different subjects and different walking speeds, as shown in Fig. 4(a) and Fig. 4(b). The most significant differences of joint angles among different subjects and walking speeds are 'shape' (i.e., trajectory maxima, minima, and timing) and gait period (i.e., time for one gait cycle). We found that some key via-points can be utilized as gait parameters G , e.g., start/end points and some extreme values in red dots with the zero joint angular velocity. Let us denote via-points as $\Theta_{via} = \{t_d^{via}, \theta_d^{via}\}_{d=1}^D$, D is the number of via-points includes the start/end points and a selection of extreme values in joint angles. For hip joint angles, 4 via-points are selected as gait parameters, $D = 4$. For knee joint angles, 5 via-points are selected as gait parameters, $D = 5$. The gait parameters $G = \{G^h, G^k\}$ with hip and knee via-points can be described as

$$G = [\Theta_{via1}^h, \dots, \Theta_{via4}^h, \Theta_{via1}^k, \Theta_{via2}^k, \dots, \Theta_{via5}^k]. \quad (3)$$

Therefore, there are 18 parameters in total for G . Note that the Gait Period (GP) is the time of the end-point of the hip/knee joint angle, i.e., $GP = t_5^{via}$. The structure of the GPM is shown in Fig. 5, the neural units for the input layer, the hidden layer and the output layer are 13, 128, and 18, respectively. Adam optimization [28] is adopted to find the optimal neural network parameters.

C. Gait Trajectory Model

The GTM is built to encode and reproduce joint angles. Two KMPs are employed to encode the hip and knee joint trajectory separately, the performance of the GTM and PVT interpolation method are compared in Section III. As the knee joint trajectory model is similar to the hip joint, here we only present the GTM for the hip joint. Assuming that the hip joint angle is denoted as

$$\theta = [\theta^h, \dot{\theta}^h]^T, \quad (4)$$

where θ^h and $\dot{\theta}^h$ represent the hip joint angle and angular velocity. T indicates the transposition of the matrix.

Denote the set of joint angles by $\{\{t_{n,m}, \theta_{n,m}\}_{n=1}^M\}_{m=1}^M$, where $t_{n,m} \in \mathbb{R}^1$ is the time and $\theta_{n,m} \in \mathbb{R}^2$ denotes joint angles. M and N represent the number of demonstrations and the length of the trajectory respectively. To estimate the probabilistic distribution of the demonstrated joint angles, GMM is employed to encode the demonstrated data and estimate the joint probability distribution $P(t, \theta)$

$$\begin{bmatrix} t \\ \theta \end{bmatrix} \sim \sum_{k=1}^K \pi_k \mathcal{N}(\mu_k, \Sigma_k), \quad (5)$$

where K denotes the number of Gaussian components, π_k , μ_k and Σ_k represent the prior probability, mean and covariance of the k^{th} Gaussian component, respectively. Thus a probabilistic reference trajectory $\{\hat{\theta}_n\}_{n=1}^N$ can be retrieved by GMR [24]

$$\hat{\theta}_n | t_n \sim \mathcal{N}(\hat{\mu}_n, \hat{\Sigma}_n), \quad (6)$$

where each $\hat{\theta}_n$ associated with t_n is described by a conditional probability distribution with mean $\hat{\mu}_n$ and covariance $\hat{\Sigma}_n$. Let us formulate a parametric hip joint trajectory comprising joint angle $\theta(t)$ and angular velocity $\dot{\theta}(t)$ as

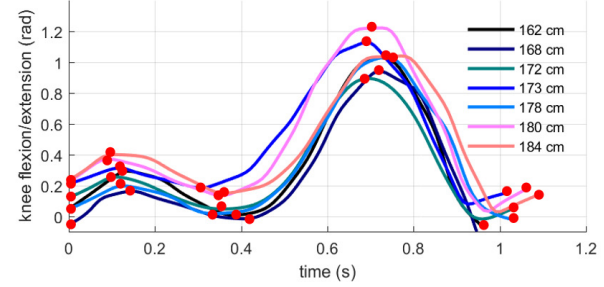
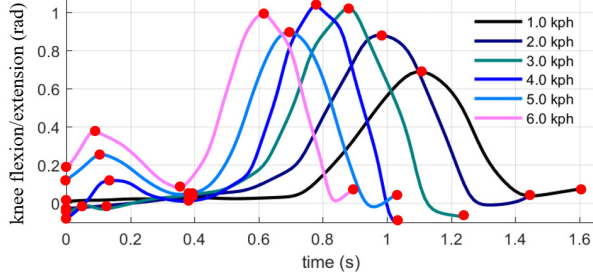
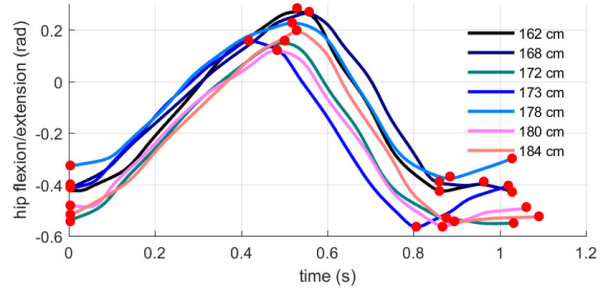
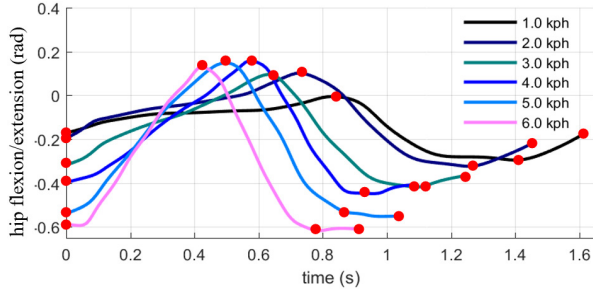
$$[\theta(t), \dot{\theta}(t)]^T = \Phi(t)^T \Omega, \quad (7)$$

where the matrix $\Phi(t) \in \mathbb{R}^{\mathcal{B} \times \mathcal{O}}$ and $\Phi(t) = [\phi(t), \dot{\phi}(t)]$, here the output dimension \mathcal{O} is 1, $\phi(t)$ is a \mathcal{B} -dimensional basis functions, $\dot{\phi}(t)$ is the first-order derivative of the $\phi(t)$. Note that we don't explicitly define the basis function $\phi(t)$ by using the kernel method proposed in [27]. $\Omega \in \mathbb{R}^{\mathcal{B} \times \mathcal{O}}$ is the weight vector. Assuming that Ω is normally distributed with mean μ_ω and covariance Σ_ω as follows $\Omega \sim \mathcal{N}(\mu_\omega, \Sigma_\omega)$. Therefore, the hip joint parametric trajectory satisfies

$$\mathcal{P}_p(\theta|t) = \mathcal{N}(\theta | \Phi(t)^T \mu_\omega, \Phi(t)^T \Sigma_\omega \Phi(t)). \quad (8)$$

Assuming that $\theta_d^{via} | t_d^{via} \sim \mathcal{N}(\mu_d, \Sigma_d)$, then

$$\mathcal{P}_d(\theta|t_d) = \mathcal{N}(\theta | \Phi(t_d)^T \mu_d, \Phi(t_d)^T \Sigma_d \Phi(t_d)). \quad (9)$$



(a) Gait patterns for one subject with different speeds.

(b) Gait patterns of one speed across different subjects.

Fig. 4. Gait patterns comparison with different subjects via varying walking speeds: (a) Joint angles from a healthy subject (176 cm, 65 kg) with different walking speeds from 1.0 kph to 6.0 kph. These joint angles can be reconstructed with the start/end points and selected extreme points (via-points in red dot); (b) Joint angles for different subjects with 3 km/h speed, the maxima, minima, and timing of hip and knee joint angles are different across subjects.

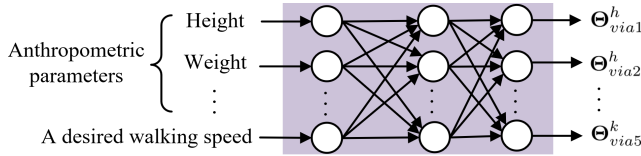


Fig. 5. The structure of the GPM, the inputs are anthropometric features and the desired walking speed, the outputs are gait parameters for the GTM.

the reference trajectory retrieved by GMR is $\mathcal{P}_r(\theta|t) = \mathcal{N}(\theta|\hat{\mu}, \hat{\Sigma})$. To match the reference trajectory formulated by (6) with the parametric trajectory and the desired via-points, and derive optimal solutions for both μ_ω and Σ_ω , the *Kullback-Leibler* divergence is employed to construct the cost function and formulate the minimization of the cost function [27] as

$$J(\mu_\omega, \Sigma_\omega) = \sum_{n=1}^N D_{KL}(\mathcal{P}_p(\theta|t_n) || \mathcal{P}_r(\theta|t_n)) + \sum_{d=1}^D D_{KL}(\mathcal{P}_p(\theta|t_d) || \mathcal{P}_d(\theta|t_d)) \quad (10)$$

The minimization of the cost function is decomposed into two sub-problems and summarized in Algorithm 1, where λ is an additional factor for $J(\mu_\omega, \Sigma_\omega)$ optimization, $\mathbb{E}(\theta(t^*))$ is the reproduction of GTM, Σ is the covariance matrix. Σ and μ can be described as

$$\Sigma = \text{blockdiag}(\hat{\Sigma}_1, \hat{\Sigma}_2, \dots, \hat{\Sigma}_{N+D}), \quad (11)$$

$$\mu = [\hat{\mu}_1^T \hat{\mu}_2^T \dots \hat{\mu}_{N+D}^T]^T. \quad (12)$$

\mathbf{K} and \mathbf{k}^* are the kernel matrix for GTM, see Appendix.

Algorithm 1 Trajectory modeling using GTM

1: Initialization

- Choose kernel $k(t_i, t_j) = e^{-h(t_i - t_j)^2}$, set the factor λ .

2: Learning from Demonstrations with GMM-GMR

- Collect demonstrations $\{\{t_{n,m}, \theta_{n,m}\}_{n=1}^N\}_{m=1}^M$.
 - Estimate the reference trajectory $\{t_n, \hat{\mu}_n, \hat{\Sigma}_n\}_{n=1}^N$.

3: Learning and prediction with via-points

- Given desired via points $\{t_d, \hat{\mu}_d, \hat{\Sigma}_d\}_{d=1}^D$.
 - *Input*: query t^* .
 - Calculate Σ, μ, \mathbf{K} and \mathbf{k}^* using (11) (14) and (15).
 - *Output*: $\mathbb{E}(\theta(t^*)) = \mathbf{k}^*(\mathbf{K} + \lambda\Sigma)^{-1}\mu$ and $\mathbb{D}(\theta(t^*)) = \frac{N+D}{\lambda} (\mathbf{k}(t^*, t^*) - \mathbf{k}^*(\mathbf{K} + \lambda\Sigma)^{-1}\mathbf{k}^{*T})$.

III. EXPERIMENTAL RESULTS AND DISCUSSION

A. Data Collection

An experiment was designed to collect gait patterns and gait parameters from healthy subjects without gait impairments. Thirty subjects (males, ages are between 20 and 41) were invited to participate in the experiment. For each subject, twelve anthropometric parameters were measured, as shown in Fig 3. Means and standard deviations of the anthropometric parameters are shown in Table I.

Subjects were instructed to walk on a treadmill with speeds from 1.0 kph to 6.0 kph at 0.5 kph increments, the duration is more than 5 minutes. As shown in Fig. 6 (a) and (b), the joint angles were recorded by Noitom Axis Neuron (an IMU based wearable Motion Capture System). To obtain the 'best fitted' gait patterns for the specified walking speeds, the gait patterns for the first and last three steps in each time were discarded. Since the gait pattern is periodic, the

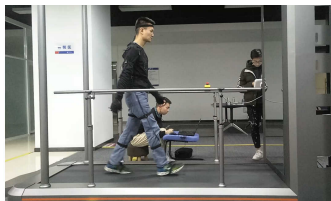
TABLE I

MEANS AND STD. OF SUBJECT'S ANTHROPOMETRIC PARAMETERS.

Anthropometric parameters	Mean	Std.
1. Body height (cm)	172.91	6.41
2. Leg length (cm)	90.58	4.24
3. Thigh length (cm)	42.9	2.34
4. Shank length (cm)	41.13	1.96
5. Ankle height (cm)	6.82	0.83
6. Foot length (cm)	25.0	0.89
7. Foot width (cm)	9.23	0.42
8. Waist circumference (cm)	82.8	6.47
9. Bi-trochanteric width (cm)	36.35	2.64
10. Maximum thigh circumference (cm)	48.72	3.81
11. Maximum shank circumference (cm)	35.81	2.04
12. Body weight (kg)	65.18	8.53



(a) Noitom Axis Neuron



(b) A healthy subject is walking on a treadmill

Fig. 6. (a) Noitom Axis Neuron; (b) Data collection from healthy subjects.

gait patterns were segmented to multiple gait cycles to build the gait database Q . For the evaluation of the GPM and GTM, twenty-four subject's anthropometric parameters and gait patterns were randomly chosen as the training dataset, and the remaining six subject's anthropometric parameters and gait patterns were chosen as the testing dataset.

B. Evaluation of the reconstructed gait patterns

The proposed approach has been tested on a lower limb exoskeleton named AIDER, which provides gait training on the treadmill. As shown in Fig. 7, AIDER is strapped to the patient's legs for movement assistance and comprises a backpack, two legs, and two shoes. For each leg, the hip flexion/extension joint and knee flexion/extension joint are actuated by DC servo motors (Maxon EC 90flat, 160 Watt, nominal speed is 2640 rpm, nominal torque is 460 mNm) in the control of high gains PID controllers, the ankle joint is an energy-storage mechanism with a spring inside that provides passive abduction/adduction and plantarflexion/dorsiflexion movement. There is an embedded computer with a real-time operating system in the backpack of the AIDER, which has a high computation speed to run algorithms. The learning of the GPM and GTM was off-line, then the GPM and GTM were imported into the embedded computer and used for gait generation for new subjects. In addition to this, the desired walking speed was specified by the therapist and sent to AIDER with anthropometric parameters via data bus before the gait training, and the reconstructed joint angles were utilized as reference joint angles for the AIDER. Subjects can maintain balance with their upper limbs and handrails while walking on the treadmill.

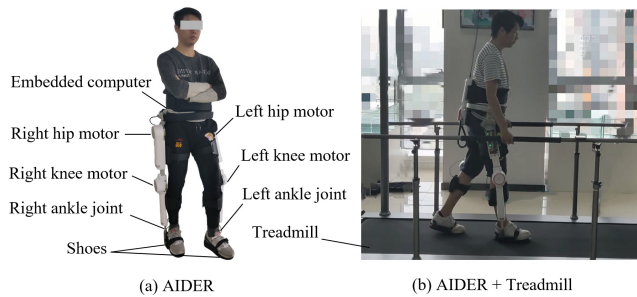


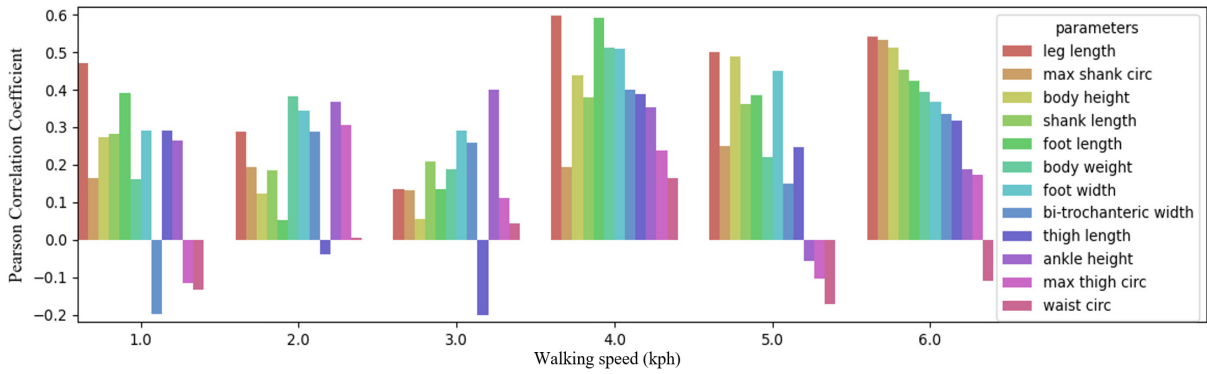
Fig. 7. Gait training on the treadmill with AIDER.

1) *Gait parameters prediction*: To find the anthropometric parameters that mainly affect the gait patterns, the Pearson's correlation coefficient [29] [30] is utilized to analyze the correlations between the twelve anthropometric parameters and gait parameters, e.g., the GP, the hip amplitude (maximum hip angle), the knee amplitude (maximum knee angle). As shown in Fig. 8, the results indicate that the anthropometric parameters that mainly affect gait parameters with high Pearson's correlation coefficients are slightly different for different walking speeds. For instance, given a walking speed at 4.0 kph, GP is positively correlated with height, hip amplitude is negatively correlated with height, and knee amplitude is negatively correlated with thigh circumference and shank circumference. This again shows the relationship between anthropometric parameters and gait parameters is complicated. Fortunately, the GPM address the problem well. As shown in Fig. 9, the GP for different subjects with varying walking speeds can be predicted with few prediction errors, as shown in Table II. Other gait parameters for different subjects and varying walking speeds can also be well predicted, as will be shown in the following section.

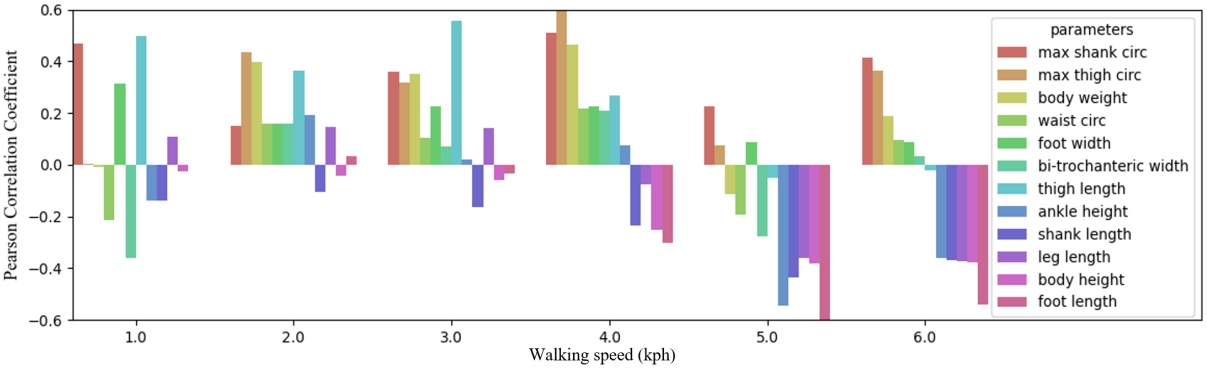
TABLE II
ERRORS BETWEEN REFERENCE GP AND PREDICTED GP.

	1.0 kph	2.0 kph	3.0 kph	4.0 kph	5.0 kph	6.0 kph
S1	-0.0560	0.0084	-0.0083	-0.0121	-0.0026	0.0114
S2	0.0639	-0.0270	0.0074	0.0051	-0.0078	-0.0021
S3	0.0501	-0.0033	-0.0160	-0.0093	-0.0047	-0.0019
S4	-0.0776	0.0096	0.0212	-0.0180	0.0097	-0.0003

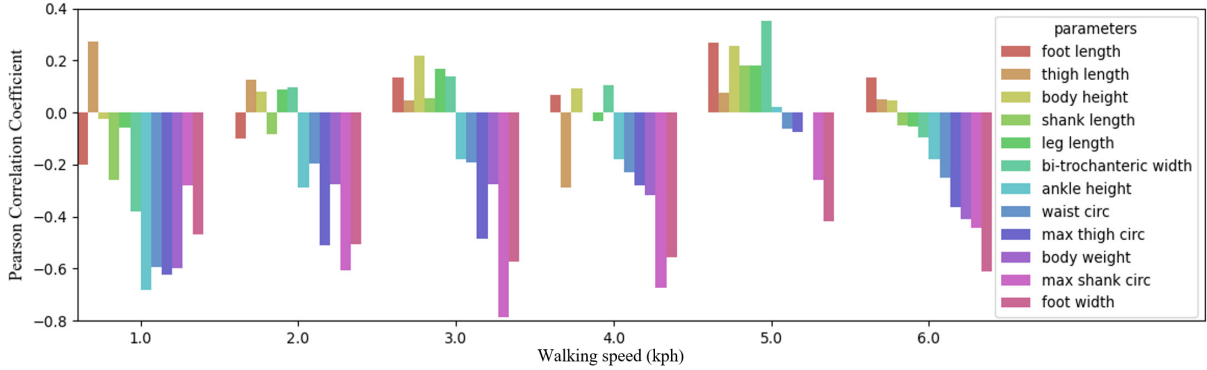
2) *Joint angles reconstruction*: The joint angles learning and reproduction for different given via-points are shown in Fig. 10. The distribution of joint angles can be learned by GMM with 10 Gaussian components, the reference trajectory can be reproduced by GMR. The GTM can reconstruct hip/knee joint angles with the demonstrated angles and different given via-points. PVT is widely used for smooth and continuous trajectory generation with given via-points, thus we compared the performance of GTM with the PVT interpolation. As shown in Fig. 11, joint trajectories reconstructed by GTM and PVT can pass through the predicted via-points. However, for the knee angle prediction for 3 kph and 4 kph walking speed, the PVT lost the 'shape' information and can not reconstruct joint angles well compared with the



(a) Pearson's correlation coefficients between anthropometric parameters and gait period.



(b) Pearson's correlation coefficients between anthropometric parameters and hip amplitude (maximum hip joint angle).



(c) Pearson's correlation coefficients between anthropometric parameters and knee amplitude (maximum knee joint angle).

Fig. 8. Pearson's correlation coefficients between anthropometric parameters and gait parameters, where 'circ' represents circumference.

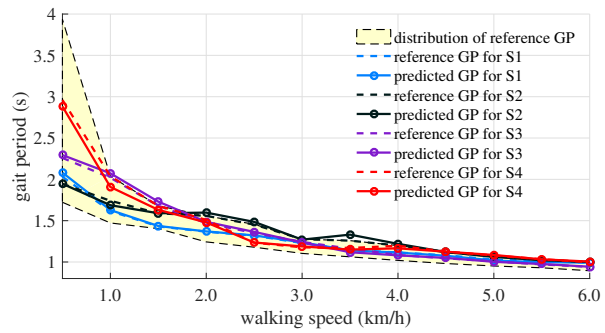


Fig. 9. Gait period prediction for different subjects with different walking speeds, the gait period is reduced with the increase of the walking speed. The dashed curves represent reference gait periods in the database, solid curves represent predicted gait periods, where subject S1 (162 cm, 58 kg), S2 (169 cm, 65 kg), S3 (176 cm, 72 kg) and S4 (183 cm, 78 kg).

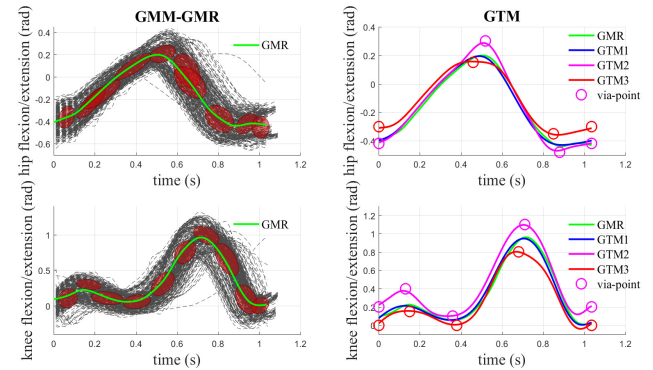


Fig. 10. GTM learning and reproduce joint angles from gait database with 3 km/h walking speed, the reference joint angles are retrieved by GMM-GMR, and joint angles with different given via-points are reconstructed by GTM, where GTM2 and GTM3 are with different given via-points.

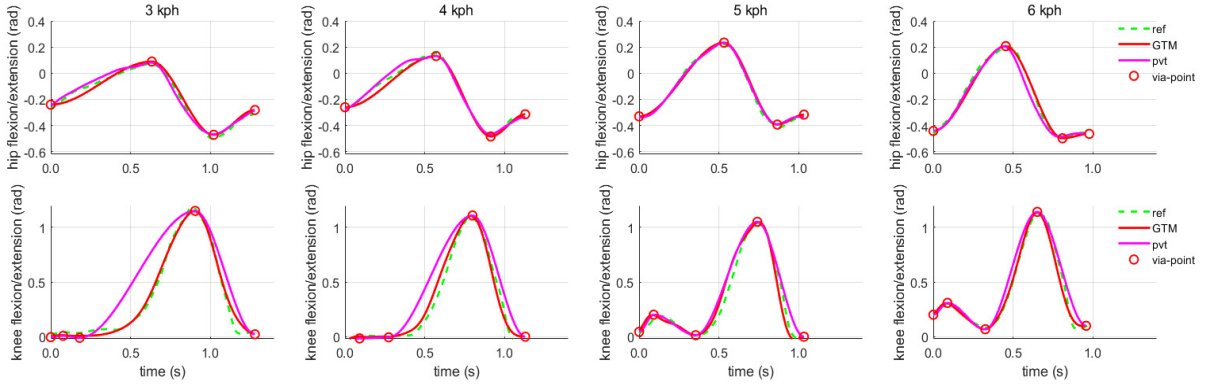


Fig. 11. Comparison of joint angles reconstruction by GTM and PVT with different walking speeds for a subject (male, 176 cm, 65 kg) from the training dataset, where the reference trajectory (i.e., the ground truth), GTM reproduction and PVT interpolation based trajectories are presented.

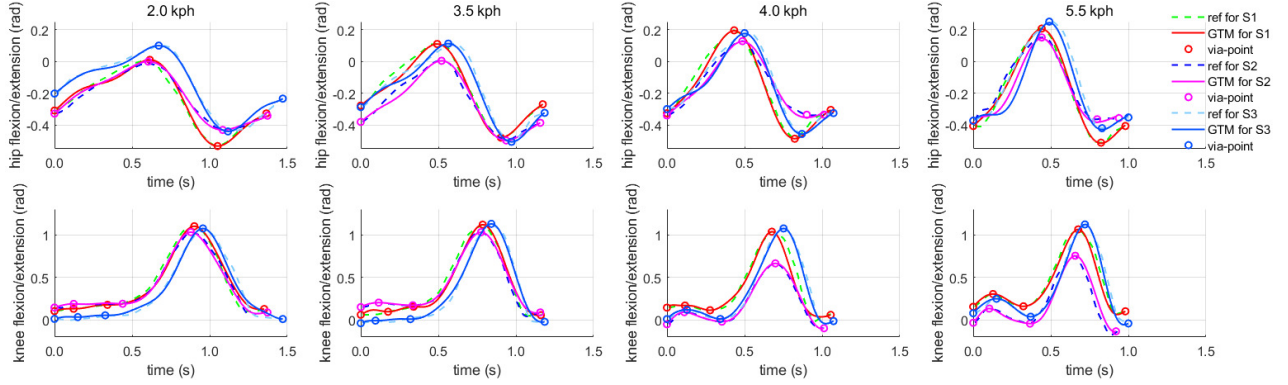


Fig. 12. Joint angles reconstruction for three subjects S1, S2, S3 from the testing dataset and four new given different walking speeds, the dashed lines represent the actual reference joint angles for each subject, the solid lines represent the predicted joint angles by the GTM.

reference joint angles, while the GTM can well reconstruct joint angles for both 3 kph and 4 kph walking speeds. The reconstruction errors were calculated by Mean Absolute Error (MAE) between reference and predicted joint angles

$$MAE = \frac{1}{N} \sum_i |\theta_i - \hat{\theta}_i|, \quad (13)$$

where θ_i and $\hat{\theta}_i$ are reference joint angles and predicted joint angles respectively, N is the number of the data point. As shown in Fig. 13, the GTM can reconstruct both hip and knee joint angles with fewer errors than the PVT, especially at low walking speeds. As shown in Fig. 12, given three subjects from testing dataset with different anthropometric parameters, the GTM can reconstruct their individualized joint angles adapt to variable speeds.

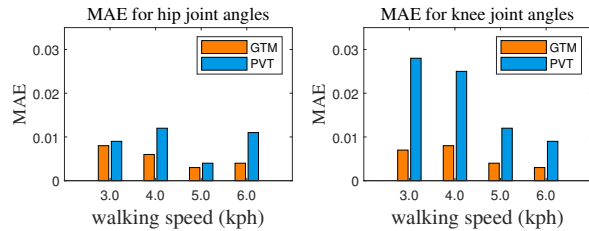


Fig. 13. MAE for hip and knee joint angles with GTM and PVT.

Although the performance of GPM and GTM is well, there is still a limitation of the work for the examination of age and gender that influence gait patterns. We only studied the anthropometric parameters for the gait patterns generation due to the limitation of the database. As the ankle joint of the AIDER is passive, we did not study the ankle joint angle reconstruction in this work. However, the framework proposed in this paper that combines neural networks and KMP is robust and generic, which can be used in future for more complicated tasks. Just add/reduce input units, output units, and network layers of the GPM if some other features are considered, the GPM and GTM also allow for secondary development with other optimization algorithms.

IV. CONCLUSIONS AND FUTURE WORKS

This paper proposed a learning-based gait planning approach for lower limb exoskeletons, which generates individualized gait patterns for different speeds. The proposed approach combines the Neural Networks and KMP for gait parameters prediction and joint angles reconstruction, the reconstructed joint angles adapt to subjects with different anthropometric parameters and varying walking speeds. The efficiency of the proposed approach has been evaluated on a lower limb exoskeleton and the experimental results indicate that the approach can generate individualized gait patterns for different subjects. In future work, we plan to expand our

database to enhance gait models, address the limitation, and incorporate gait analysis methods to apply to more scenarios.

APPENDIX

In Algorithm 1, \mathbf{K} is a matrix which can be described as

$$\mathbf{K} = \begin{bmatrix} \mathbf{k}(t_1, t_1) & \mathbf{k}(t_1, t_2) & \cdots & \mathbf{k}(t_1, t_{N+D}) \\ \mathbf{k}(t_2, t_1) & \mathbf{k}(t_2, t_2) & \cdots & \mathbf{k}(t_2, t_{N+D}) \\ \vdots & \vdots & \ddots & \vdots \\ \mathbf{k}(t_{N+D}, t_1) & \mathbf{k}(t_{N+D}, t_2) & \cdots & \mathbf{k}(t_{N+D}, t_{N+D}) \end{bmatrix}, \quad (14)$$

and the kernel matrix k^* can be described as

$$\mathbf{k}^* = [\mathbf{k}(t^*, t_1) \ \mathbf{k}(t^*, t_2) \ \cdots \ \mathbf{k}(t^*, t_{N+D})]. \quad (15)$$

Note that the kernel $k(t_i, t_j) = \phi(t_i)^T \phi(t_j)$, and the kernel matrix can be determined by

$$\mathbf{k}(t_i, t_j) = \Phi(t_i)^T \Phi(t_j) = \begin{bmatrix} k_{tt}(i, j) \mathbf{I}_O & k_{td}(i, j) \mathbf{I}_O \\ k_{dt}(i, j) \mathbf{I}_O & k_{dd}(i, j) \mathbf{I}_O \end{bmatrix}, \quad (16)$$

where

$$k_{tt}(i, j) = k(t_i, t_j),$$

$$k_{td}(i, j) = \frac{k(t_i, t_j + \delta) - k(t_i, t_j)}{\delta},$$

$$k_{dt}(i, j) = \frac{k(t_i + \delta, t_j) - k(t_i, t_j)}{\delta},$$

$$k_{dd}(i, j) = \frac{k(t_i + \delta, t_j + \delta) - k(t_i + \delta, t_j) - k(t_i, t_j + \delta) + k(t_i, t_j)}{\delta^2}.$$

ACKNOWLEDGMENT

This work was supported by National Key Research and Development Program of China (No. 2017YFB1302300) and National Natural Science Foundation of China (NSFC) (No. 6150020696, 61503060).

REFERENCES

- [1] S. Jezernik, G. Colombo, and M. Morari, "Automatic gait-pattern adaptation algorithms for rehabilitation with a 4-dof robotic orthosis," *IEEE Transactions on Robotics & Automation*, vol. 20, no. 3, pp. 574–582, 2004.
- [2] A. Esquenazi, M. Talaty, A. Packel, and M. Saulino, "The rewalk powered exoskeleton to restore ambulatory function to individuals with thoracic-level motor-complete spinal cord injury," *Am J Phys Med Rehabil*, vol. 91, no. 11, pp. 911–921, 2012.
- [3] L. E. Miller, A. K. Zimmermann, and W. G. Herbert, "Clinical effectiveness and safety of powered exoskeleton-assisted walking in patients with spinal cord injury: systematic review with meta-analysis," *Medical Devices*, vol. 9, p. 455, 2016.
- [4] C. Tefertiller, K. Hays, J. Jones, A. Jayaraman, C. Hartigan, T. Bushnik, and G. Forrest, "Initial outcomes from a multicenter study utilizing the indigo powered exoskeleton in spinal cord injury," *Topics in Spinal Cord Injury Rehabilitation*, 2017.
- [5] H. Kawamoto, S. Lee, S. Kanbe, and Y. Sankai, "Power assist method for hal-3 using emg-based feedback controller," in *IEEE International Conference on Systems, Man and Cybernetics*, vol. 2, 2003, pp. 1648–1653.
- [6] A. M. Barthuly, R. W. Bohannon, and W. Gorack, "Gait speed is a responsive measure of physical performance for patients undergoing short-term rehabilitation," *Gait & posture*, vol. 36, no. 1, pp. 61–64, 2012.
- [7] N. M. Peel, S. S. Kuys, and K. Klein, "Gait speed as a measure in geriatric assessment in clinical settings: a systematic review," *The Journals of Gerontology: Series A*, vol. 68, no. 1, pp. 39–46, 2013.
- [8] M. U. Quiben and H. P. Hazuda, "Factors contributing to 50-ft walking speed and observed ethnic differences in older community-dwelling mexican americans and european americans," *Physical therapy*, vol. 95, no. 6, pp. 871–883, 2015.

- [9] J. E. Graham, G. V. Ostir, S. R. Fisher, and K. J. Ottenbacher, "Assessing walking speed in clinical research: a systematic review," *Journal of evaluation in clinical practice*, vol. 14, no. 4, pp. 552–562, 2008.
- [10] H. J. van Hedel, V. Dietz, and A. Curt, "Assessment of walking speed and distance in subjects with an incomplete spinal cord injury," *Neurorehabilitation and neural repair*, vol. 21, no. 4, pp. 295–301, 2007.
- [11] H. Hsiao, T. M. Zabielski Jr, J. A. Palmer, J. S. Higginson, and S. A. Binder-Macleod, "Evaluation of measurements of propulsion used to reflect changes in walking speed in individuals poststroke," *Journal of biomechanics*, vol. 49, no. 16, pp. 4107–4112, 2016.
- [12] E. Duim, M. L. Lebrão, and J. L. F. Antunes, "Walking speed of older people and pedestrian crossing time," *Journal of Transport & Health*, vol. 5, pp. 70–76, 2017.
- [13] G. Kwakkel and R. C. Wagenaar, "Effect of Duration of Upper- and Lower-Extremity Rehabilitation Sessions and Walking Speed on Recovery of Interlimb Coordination in Hemiplegic Gait," *Physical Therapy*, vol. 82, no. 5, pp. 432–448, 05 2002.
- [14] A. Schmid, P. W. Duncan, S. Studenski, S. M. Lai, L. Richards, S. Perera, and S. S. Wu, "Improvements in speed-based gait classifications are meaningful," *Stroke*, vol. 38, no. 7, pp. 2096–2100, 2007.
- [15] Y. Yun, H. C. Kim, S. Y. Shin, J. Lee, A. D. Deshpande, and C. Kim, "Statistical method for prediction of gait kinematics with gaussian process regression," *Journal of Biomechanics*, vol. 47, no. 1, pp. 186–192, 2014.
- [16] S. Ren, W. Wang, Z. G. Hou, X. Liang, J. Wang, and L. Peng, "Anthropometric features based gait pattern prediction using random forest for patient-specific gait training," pp. 15–26, 2018.
- [17] S. Ren, W. Wang, Z. G. Hou, B. Chen, X. Liang, J. Wang, and L. Peng, "Personalized gait trajectory generation based on anthropometric features using random forest," *Journal of Ambient Intelligence and Humanized Computing*, Jul 2019.
- [18] M. Florent, L. Fabien, and A. Stéphane, "Lower limb sagittal gait kinematics can be predicted based on walking speed, gender, age and bmi," *Scientific Reports*, Jul 2019.
- [19] H. B. Lim, T. P. Luu, K. H. Hoon, and K. H. Low, "Natural gait parameters prediction for gait rehabilitation via artificial neural network," in *IEEE/RSJ International Conference on Intelligent Robots & Systems*, 2010.
- [20] S. Y. Shin and S. James, "An online transition of speed-dependent reference joint trajectories for robotic gait training," in *IEEE International Conference on Rehabilitation Robotics*, 2019, pp. 983–987.
- [21] L. Trieu Phat, K. H. Low, Q. Xingda, H. B. Lim, and K. H. Hoon, "An individual-specific gait pattern prediction model based on generalized regression neural networks," *Gait & Posture*, vol. 39, no. 1, pp. 443–448, 2014.
- [22] B. Koopman, E. H. F. V. Asseldonk, and H. V. D. Kooij, "Speed-dependent reference joint trajectory generation for robotic gait support," *Journal of Biomechanics*, vol. 47, no. 6, pp. 1447–1458, 2014.
- [23] X. Wu, D. X. Liu, L. Ming, C. Chen, and H. Guo, "Individualized gait pattern generation for sharing lower limb exoskeleton robot," *IEEE Transactions on Automation Science & Engineering*, vol. 15, no. 4, pp. 1459–1470, Oct 2018.
- [24] S. Calinon, "A tutorial on task-parameterized movement learning and retrieval," *Intelligent Service Robotics*, vol. 9, no. 1, pp. 1–29, 2016.
- [25] R. Lioutikov, G. Neumann, G. Maeda, and J. Peters, "Learning movement primitive libraries through probabilistic segmentation," *The International Journal of Robotics Research*, vol. 36, no. 8, pp. 879–894, 2017.
- [26] A. Paraschos, "Robot skill representation, learning and control with probabilistic movement primitives," Ph.D. dissertation, Technische Universität, 2017.
- [27] Y. Huang, L. Roza, J. Silvério, and D. G. Caldwell, "Kernelized movement primitives," *The International Journal of Robotics Research*, vol. 38, no. 7, pp. 833–852, 2019.
- [28] D. P. Kingma and J. Ba, "Adam: A method for stochastic optimization," *International Conference on Learning Representations*, 2014.
- [29] J. Rodgers and W.A. Nicewander, "Thirteen ways to look at the correlation coefficient," *The American Statistician*, vol. 42, pp. 59–66, 1998.
- [30] A. G. Asuero, A. Sayago, and A. G. González, "The correlation coefficient: An overview," *Critical Reviews in Analytical Chemistry*, vol. 36, no. 1, pp. 41–59, 2006.